The J/Ψ as a probe of Quark-Gluon Plasma

Luciano MAIANI
Università di Roma "La Sapienza" and
INFN. Roma. Italy

Lectures given at the International School of Subnuclear Physics
29 August – 7 September 2004
Ettore Majorana Centre for Scientific Culture
Erice, Trapani, Italy

Abstract

Anomalous suppression of J/Ψ in the collisions of Heavy Nuclei is considered to provide reliable indications for the formation of a fire-ball of deconfined quarks and gluons. After a brief review of hadron thermodynamics at high energy, I illustrate recent calculations of J/Ψ absorption in hadronic matter and the ensuing analysis of the data obtained at the CERN SPS by the NA50 Collaboration. Assuming the existence of a limiting hadron temperature, as indicated by the hadron level spectrum, one concludes that normal hadronic matter cannot explain the observed suppression in higher centrality collisions.

Introduction

Confinement means that the heavy quarks in a c-cbar pair are bound by an asymptotically constant attractive force (i.e. a linearly rising potential). This is what happens in normal vacuum.

Several theoretical arguments suggest that by increasing the temperature, normal vacuum gives rise to a new phase where quarks and gluons are not confined in hadron bags. In the deconfined phase, the attractive force between c and c-bar is screened by the Quark-Gluon Plasma (QGP). Charmonia bound states "melt" as temperature rises, starting from the less bound higher resonances down to the more deeply bound lower states. Thus, te onset of J/Ψ suppression in relativistic heavy ion collisions would signal the formation of QGP, a suggestion originally made by T. Matsui and H. Satz[1].

The method can work, however, only if we are able to control all other sources of J/Ψ absorption in heavy ion collisions, both nuclear and hadronic[2]. To this aim, several calculations of the J/Ψ dissociation cross-sections have been performed, e.g. for the process:

$$h + J/\Psi \rightarrow D + \overline{D}$$
$$(h = \pi, \rho, \ldots)$$

J/ Ψ dissociation by hadrons was originally believed to be very small, on the basis of perturbative QCD calculations, but more recent studies have shown its importance.

I will report on the results of a recent calculation by our group[3] and apply them to the NA50 data obtained at the SPS.

The present Lectures give a "bottom up" presentation[4], going (slowly) from low to high temperature. The 1st lecture contains an elementary introduction to the basic concepts and in the 2nd lecture I shall present the results of our calculations and their application to the data taken at the CERN SPS by the NA50 Collaboration[5].

The main issue I will address is: ***did quark-gluon plasma show up at the SPS?***

On the basis of our results, I conclude: ***yes, most likely !!***

But we need to know better...and to study QGP more, at RHIC and LHC.

Before closing the Introduction, I would like to express my gratitude to U. Heinz, U. Wiedemann and F. Becattini for interesting discussions. The help of F. Becattini in constructing the 2004 hadron level spectrum is gratefully acknowledged. Finally, I want to thank my younger collaborators F. Piccinini, A. Polosa and V. Riquer, who introduced me to the problem of J/Ψ dissociation and shared the enthusiasm of exploring the new (for us) world of heavy ion collisions.

LECTURE 1

Summary

1. *A simple view of the collisions*
2. *Does the fireball thermalise?*
3. *Hadron gas*
4. *Hagedorn gas, the phase transition from below*
5. *Deconfined Quarks and Gluons*
6. *Debye screening*
7. *Summing up*

1. A simple view of the collisions

Snapshots of the high-energy collision of two (equal) heavy ions, taken in the c.o.m. frame before and after the collision, would look like the cartoons in Fig.1. The center of mass energies of the projectiles are 8.5 GeV/A at the SPS, 100 GeV/A at RHIC and will be 2.5 TeV/A at the LHC.
Nuclei are compressed in the direction of flight by the relativistic contraction, the closest distance of approach (impact parameter) is indicated by *b*.
The value of *b* in each collision can be measured by observing the energy carried by the fragment of nucleus which has gone on unperturbed, represented with a solid shape in Fig. 1. In the SPS, fixed target, experiments the unperturbed fragment of the projectile nucleus goes forward and its energy is measured in NA50 by a Zero Degree Calorimeter. The fragment has the same Energy/A ratio as the original projectile, thus we can get A from the energy and deduce its size, i.e. *b*, from nuclear models (see below).

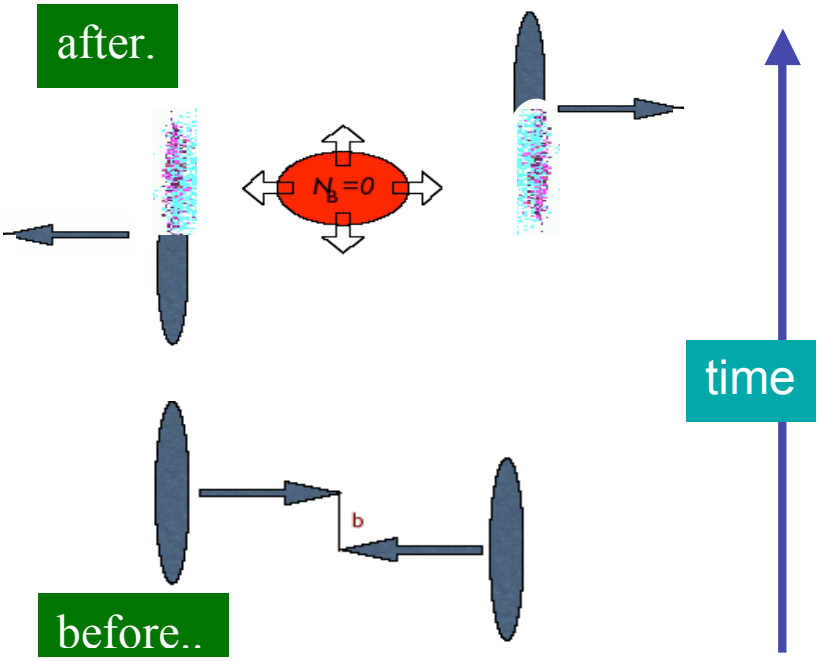

Fig. 1.1. Snapshot of a relativistic heavy ion collision, center of mass frame.

The overlap region of the two nuclei after collision is represented with a fuzzy shape: nucleons are now unbound and mixed with the forward and backward fragments of individual collisions.

Hadrons produced in the central region of the rapidity plateau form a fireball which expands rapidly under the pressure exerted by the momentum of the inner particles..
The central plateau is separated from the fragmentation region by a rapidity interval

which increases with the c.o.m. energy. Therefore, the central region is more and more baryon number free. The fireball starts as a state of dense hadronic matter with a transverse size which we denote by l (l =2R-b where R is the radius of each nucleus).

Shortly after the collision, at a time τ_0 = 0.1-1 fm/c, the energy density of the fireball for central collsions, b=0, can be estimated in terms of the particles produced in elementary nucleon-nucleon collision[6]:

$$\varepsilon_{central} = \frac{A}{S}(\frac{dE}{dy})\frac{1}{c\tau_0} \tag{1.1}$$

here A/S is the average baryon number surface density of the incoming nuclei while the energy per unit rapidity (per nucleon-nucleon collision), can be estimated at the SPS according to:

$$\frac{dE}{dy} = \frac{dN_{ch}}{dy}(1+\frac{N_{neutrals}}{N_{ch\,\mathrm{arg}\,ed}}) < E > \cong 3\cdot 1.5\cdot 400\,MeV = 1.8GeV \tag{1.2}$$

For central Pb-Pb collision, one has:

$$\frac{A}{S} = \frac{A}{\pi R^2} = \frac{A^{1/3}}{\pi r_0^{\ 2}} = 1.5\,fm^{-2}(for: Pb)$$

For collisions with a generic impact parameter, the baryon density per unit surface is reduced by a geometrical factor:

$$\frac{A(b)}{S(b)} = \frac{A(0)}{S(0)}g(b)$$

where g(b) is the nucleon number density per unit area, averaged over the region of overlap of the colliding nuclei:

$$g(b) = \frac{\pi}{2}[\frac{(1-b/2R)^2(1+b/4)}{\arccos(b/2R) - b/2R\sqrt{1-b^2/4R^2}}] \tag{1.3}$$

For Pb-Pb collisions, R= 6 fm and g(b) decreases from 1 to about 0.6 when b goes from 0 (central collisions) *to* b=8 fm. The latter value corresponds to a transverse diameter of the fireball: l=2R-b=4 fm where the interestingly central collisions begin, as we shall see in Lecture 2. From the estimates above, we obtain

$$\begin{aligned} \varepsilon &= 1.6GeVfm^{-3}(\frac{1\,fm}{\tau_0})\cdots(l = 4\,fm) \\ \varepsilon &= 2.7GeVfm^{-3}(\frac{1\,fm}{\tau_0})\cdots(l = 12\,fm) \end{aligned} \tag{1.4}$$

2. **Does the fireball thermalise?**

Particles produced in the primary collisions are mainly pions, with an average energy of 400 MeV each. If the density of the early fireball is sufficiently high, pions will scatter many times off each other and relax to a state with some definite temperature, T. For $\tau_0 < 1$fm/c and $l = 4$fm, we can estimate an average initial density: $\rho > 4$ fm^{-3}. Taking a typical strong interaction cross section: $\sigma \cong 40\text{mb} = 4\text{fm}^{-2}$, we get the mean free path:

$$\lambda^{-1} = \rho\sigma \geq 40mb \cdot 4\, fm^{-3} = 16\, fm^{-1};$$

$$\lambda \leq 0.06\, fm$$

λ is much smaller than the size of the fireball produced (a few Fermi). Thermal equilibrium is a reasonable guess.

Some words of caution are appropriate here. Pions at zero momentum have a vanishing interaction since they are the quasi-Goldstone-bosons of chiral symmetry. Calculations based on chiral perturbation theory provide cross sections that could be much smaller than what estimated above, and predict no thermalization at all[7]. However, if the original particles have an average energy E= 400 MeV, with random distributed directions the average center of mass energy in the pion-pion system is about 560MeV ($\langle s \rangle = 2E^2$) and are rather far from the soft pion limit for Chiral perturbation Theory to be applicable. As an alternative, we may compute the P-wave pion-pion cross section using a Breit-Wigner formula for the $\rho(770)$, to find $\sigma_\rho(560\text{MeV}) \sim 33$ mb. If we add an S-wave resonance, $\sigma(480)$ with $\Gamma \sim 300$ MeV, as suggested by recent data[8], we obtain a total cross section of about 50 mb, in line with the previous estimate.

What about experiment? The hadrons that are observed originate at a later time, the so-called freeze-out time, when the expansion of the fireball has reduced the density such that the hadrons do not interact anymore among themselves. Coherently with the thermalization assumption, hadrons at freeze-out exibit a thermal distribution[9], with T=170-180 MeV.

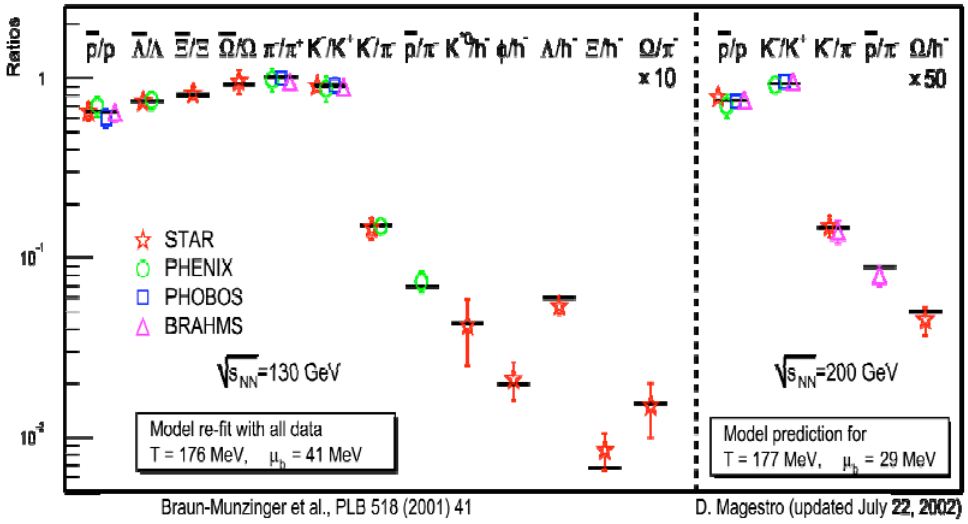

Fig. 2.1 Hadron abundances and thermdynamical fits at RHIC.

3. **Hadron gas**

At thermal equilibrium and low energies, we describe the fireball as a gas made by hadron resonances. Each particle species is treated as a free particle. Interactions are rather introduced in the form of resonances which appear at increasing energies: we have pions only at low energy, then kaons, etas, (i.e. the strange quark flavour) then ρ, ω, ϕ, K*, etc. (see e.g. Ref.[10]).

The thermodynamical partition function, Z is easily obtained if we know the hadronic gas composition, i.e. the density of hadronic level as a function of the mass:

$$\begin{aligned} &\ln Z = \int \rho(m) dm [V \int \frac{d^3 p}{(2\pi)^3} \ln(z_i)]; \\ &\ln(z_i) = \pm \ln(1 \pm e^{+\mu_i} e^{-\beta E_i(p)}); (+ = fermions, - = bosons) \end{aligned} \tag{3.1}$$

$$\rho(m) = \sum_i (2J+1) N_{ch} \delta(m - m_i) \tag{3.2}$$

(β=1/T, μ=chemical potential, k=Boltzmann's constant=1) and N_{ch} represents the charge multiplicity (3 for pions). For simplicity, in what follows we assume vanishing chemical potential. This is appropriate for the fireball produced in the central region of very high energy collisions. It is a rough approximation at SPS energies, getting better and better at RICH and LHC.

In the Boltzmann limit all exponents are <<1, so that: $\ln z \approx e^{+\mu} e^{-\beta E}$. The energy density of the hadron gas and the average species abundances are obtained from the partition function as usual:

$$\begin{aligned} &\frac{U}{V} = \varepsilon(T,\mu) = -\frac{\partial \ln Z}{\partial \beta}; \\ &n_i = \frac{\partial \ln Z}{\partial \mu_i} \end{aligned}$$

It is convenient to introduce the ratio of the energy density to that of a gas made by one specie of spin zero, massless bosons. We call N_{eff} the energy density thus normalized:

$$\begin{aligned} &N_{eff}(T) = \frac{\varepsilon(T)}{\varepsilon_o(T)}; \\ &\varepsilon_o(T) \equiv \frac{T^4 \pi^2}{30} \approx 0.33 T^4 \end{aligned} \tag{3.3}$$

Justifying its name, N_{eff} gives the number of degrees of freedom that are "active" at temperature T. At low temperatures, of the order of 150 MeV, one would expect only

pions, namely N_{eff}~3. However, in spite of higher mass, higher resonances contribute significantly to the energy density even at these temperatures, because of their increasing spin and charge multiplicities, as we discuss in the next Section.

4. Hagedorn gas: the phase transition from below

The central ingredient of the fireball thermodynamics is the density of the hadron levels, ρ(m). Of course, we are unable to compute it from first principles, at present. Repeating the exercise found in Ref.[10], I report in Fig. 4.1, black solid curve, a

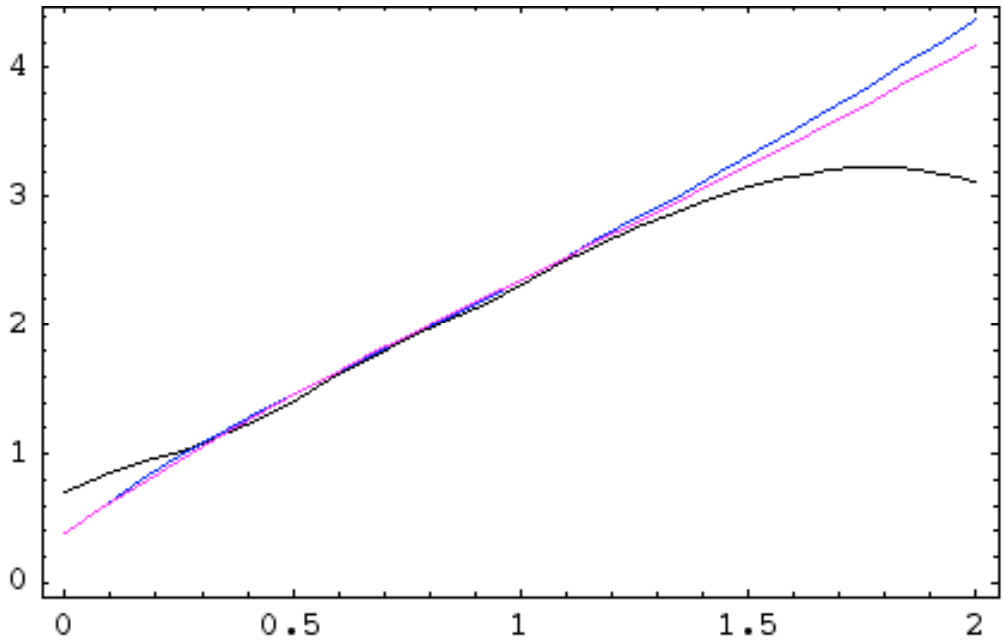

Fig. 4.1. Hadron level density functions (see text). In ordinates, the values of $\log_{10}[\rho(m)]$ are reported, with m in GeV and ρ in GeV^{-1}. For the meaning of the different curves, see text.

determination of the "experimental" level density, $\rho_{2004}(m)$ corresponding to the hadron levels listed in the Particle Data Book of 2004. Pions are not included. For the other particles, each delta-function in eq.(3.2) is smeared out in a gaussian to get a regular behaviour:

$$\delta(m - m_{res}) \to \frac{1}{\sigma\sqrt{2\pi}} e^{-\frac{(m-m_{res})^2}{2\sigma^2}}$$

with 200 MeV resolution. The level density ρ_{2004} drops for masses above approximately 1.5 GeV. This is probably because we are unable to identify highly excited resonances with increasing angular momentum and increasingly large widhts. However, in the region where we can reasonably assume that we know almost all the hadronic levels, the trend supports an exponentially increasing density, as predicted by

Hagedorn, in the prehistory of modern hadron theory, on the basis of his bootstrap principle. The exponential rise of ρ(m) is supported by hadron models based on quarks (e.g. the bag model).

The blue line in Fug. 4.1 was obtained in ref.[10] by a fit of the smeared data from the 1996 Particle Data Group with a theoretical level density of the form:

$$\rho(m) = C(m_0^2 + m^2)^{-3/2} e^{+m/T_H} \tag{4.1}$$

The power -3/2 of the pre-exponential factor is predicted by Hagedorn's "bootstrap principle" and it fits well the data. The resulting parameters are:

$$\begin{aligned} &C = 0.7 GeV^2; m_0 = 0.66 GeV; \\ &T_H = 158 MeV \end{aligned} \tag{4.2}$$

The value of T_H thus obtained is in agreement with the original determination by Hagedorn, which was based on the p_T cutoff observed in the distribution of the pions produced in hadronic collisions. However, T_H is too low to comply with the temperatures obtained from hadronic distribution at freeze-out, which we have seen to be in the range 170-180 MeV, and also with the lattics QCD results (see below) which indicate a transition temperature around 170 MeV.

However, T_H is not so well determined by the mass distribution of the observed resonances, due to the falling of the black curve. We can obtain a good fit with a larger temperature by readjusting the coefficients of the pre-exponential terms. The purple curve shows the result[3] for:

$$\begin{aligned} &C = 2.55 GeV^2; m_0 = 1.01 GeV; \\ &T_H = 180 MeV \end{aligned} \tag{4.3}$$

The exponentially rising spectrum leads to a limiting temperature for the hadronic matter, equal to T_H.

Intuitively, this can be understood as follows. An increase of the energy of the gas gives rise to two competing effects: increase of the average energy of the particles present in the gas, thereby increasing the temperature, increase of the number of species present in the gas, by creating heavier particles. With a spectrum limited in mass, the first mechanisms takes over at large temperatures and leads to the T^4 behaviour of the energy of a gas made by a fixed number of species of relativistic particles. If the level density increases exponentially, however, the second mechanisms dominates more and more and at some point it will be impossible to increase the temperature further, since any newly provided energy is spent in creating new particles.

The argument is well exemplified by Fig. 4.2. The lowest red curve gives the contributions of pions alone, flattening at the value 3. The next higher, red, curve gives N_{eff} for a hadron gas made by the pseudoscalar and vector nonets. Here, ρ(770) and ω(770) make a sizeable contributon, nothwitstanding that the values of their masses are quite larger than T. Still higher is N_{eff} computed with ρ_{2004} (green curve), while, finally the blue curve represents N_{eff} for the Hagedorn gas with the parameters given in eq.(4.3), diverging at T_H=180 MeV.

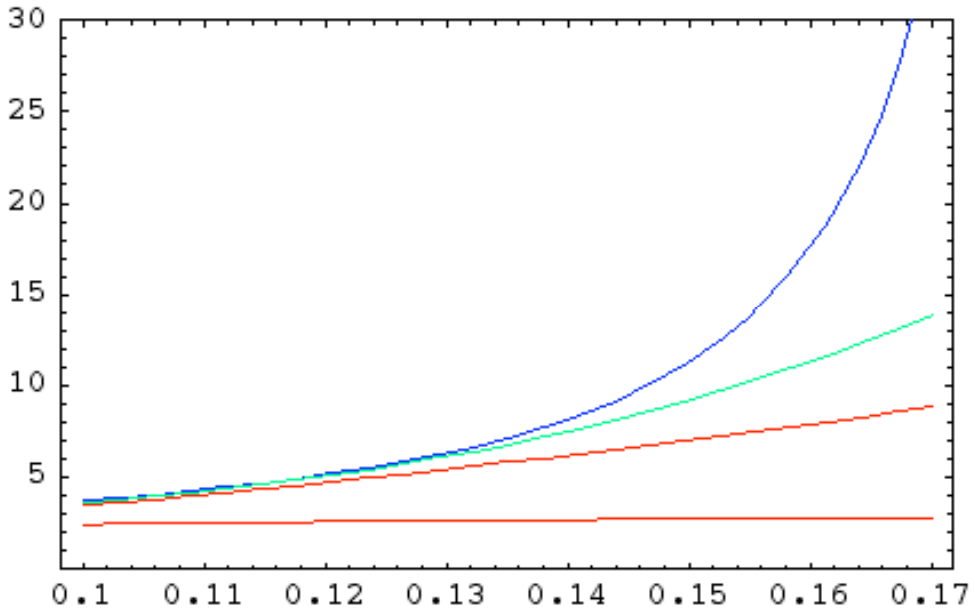

Fig. 4.2. The behavior of N_{eff}, Eq. (3.3), vs. temperature (GeV) and different hadron gases. Red lowest curve: pions; red higher curve: pseudoscalar and vector mesons; green curve: all particles in Particle Data Group 2004, with the smeared level density $\rho_{2004}(m)$; blue curve: Hagedorn gas with T_H=180 MeV.

The existence of a limiting temperature can be seen at once from the fact that the partition function:

$$Z = \sum \rho(m) e^{-\frac{m}{T}} \propto \sum m^{-k} e^{+m(\frac{1}{T_H} - \frac{1}{T})} \tag{4.4}$$

does not converge for $1/T<1/T_H$. In more recent times, looking at the same formula *from below*, the Hagedorn temperature has been interpreted as the transition to a new phase of matter[11].

This is easily seen by computing the behaviour of the thermodynamical functions while approaching T_H from below. We use the non-relativistic Boltzmann approximation, since the critical behaviour is determined by the high masss part of the spectrum, m>>T, to find ($\beta=1/T$, $\beta_C=1/T_H$):

$$\ln Z = \frac{V}{(2\pi\beta)^{3/2}} \int dm \frac{C}{(m_0^2 + m^2)^{3/2}} m^{3/2} e^{-m(\beta-\beta_c)} \approx V[A(\beta-\beta_c)^{1/2} \int_{E_0(\beta-\beta_c)}^{+\infty} dx x^{-3/2} e^{-x} + reg.]$$

where A is some constant and "reg." represents terms analytic at β_c. The integral is evaluated as follows:

$$\int_{E_0(\beta-\beta_c)}^{+\infty} dx x^{-3/2} e^{-x} = -2 \int_{E_0(\beta-\beta_c)}^{+\infty} dx x^{-1/2} e^{-x} + \frac{2}{E_0(\beta-\beta_c)^{1/2}} \approx -2 \int_0^{+\infty} dx x^{-1/2} e^{-x} + \frac{2}{E_0(\beta-\beta_c)^{1/2}}$$

so that we find, in conclusion, for pressure and for energy density :

$$P = \frac{\ln Z}{V} = reg. - 2A(\beta - \beta_C)^{1/2};$$
$$\varepsilon = -\frac{\partial}{\partial \beta} \ln Z \propto (\beta - \beta_C)^{-1/2}; \tag{4.5}$$

Near the critical point, the hadron gas is very soft: the velocity of sound vanishes at β_C:

$$v^2 = \frac{dP}{d\varepsilon} \propto (\beta - \beta_C) \tag{4.6}$$

The behavior of ε is quite reminiscent of the critical behaviour near a second order phase transition, which Cabibbo and Parisi interpreted as quark and gluon de-confinement. However, there are several differences with respect to a second order phase transition. Until now we have considered poinlike particles only. If one introduces a finite radius of the hadron levels, the behaviour becomes less critical (see again ref.[10]). In fact, we could rather be in presence of a smooth cross-over from the hadron gas state to the liberated quark and gluon plasma.

5. Order parameters for the phase transition

The order parameter for the deconfinement transition, in the pure gauge system without fermions, is the Wilson- Polyakov loop:

$$L = < \exp(-F_{Q\bar{Q}}/T) > \tag{5.1}$$

F is the free energy of a pair of static point sources (heavy quarks) at distance r. F and L have the limiting behaviours for $r \to \infty$:

$T<T_c$: $F \propto r \to \infty$, **$L \to 0$** confinement
$T>T_c$: $F \to 0$, **$L \to$ Const.$\neq 0$** deconfinement
Fig. 5.1 shows indeed a rapid rise of L at the critical temperature[12].

According to many indications, chiral symmetry is restored in the deconfined phase, indeed calculations support a drop to zero of the chiral symmetry order parameter, $< \bar{\psi}\psi >$, correlated to the raising of L , as shown in Fig. 5.2.

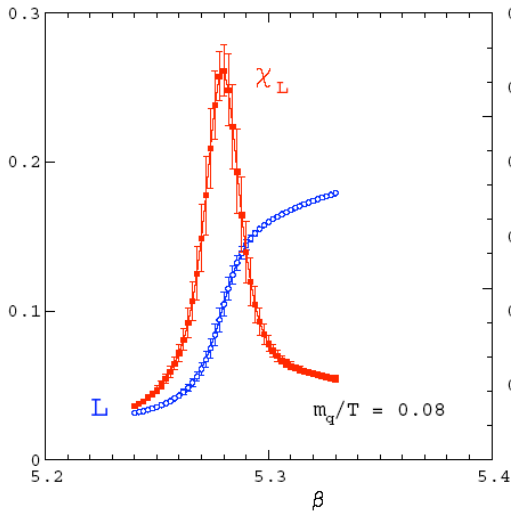

Fig. 5.1. Lattice QCD calculation of the behaviour of the Polyakov loop, Eq. (5.1), as function of Temperature (blue curve). Ref.[12].

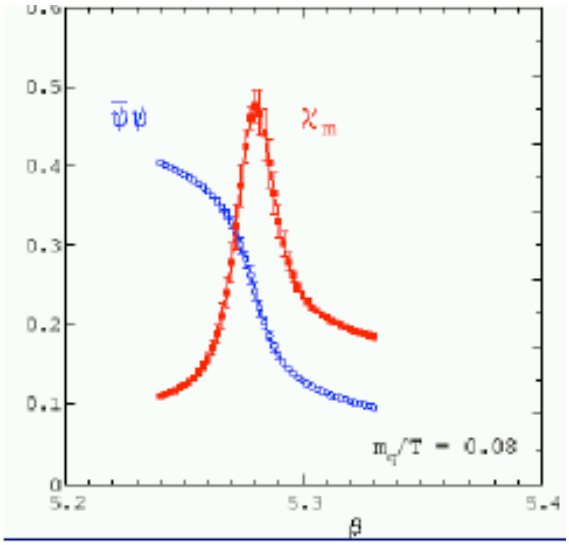

Fig. 5.2. Lattice QCD calculation of the behavior of the chiral order parameter as function of temperature (blue curve). Ref.[12].

Lattice QCD calculations indicate a first order phase transition for the pure gauge system. In the presence of quarks, it is not yet clear if the transition stays, or if it attenuates in a simple crossover, a rapid but continuous transition between a gas of hadrons and a gas of quarks and gluons. According to recent speculations, the transition would exist for non vanishing chemical potential, to stop at a tricritical point, where all phases coexist, see point E in Fig. 5.3.

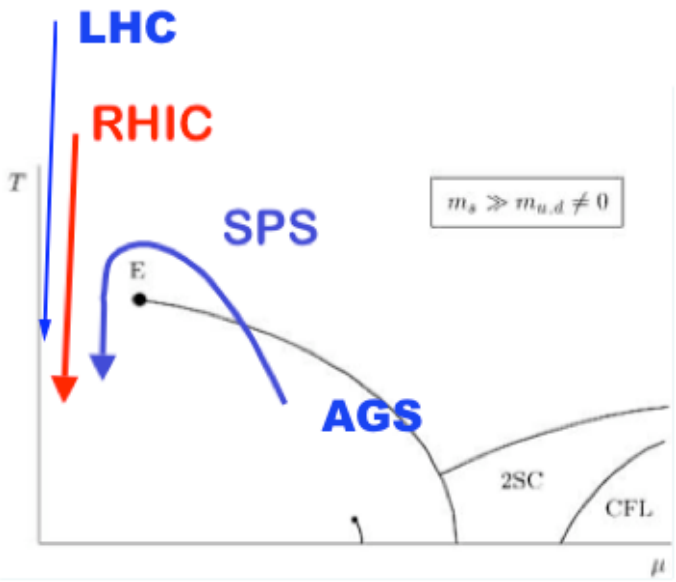

Fig. 5.3. Schematic view of predicted and/or hypothesized phase regions of hadronic matter.

A rapid increase in the energy density is shown by lattice QCD calculations with unquenched quarks (see again F. Karsch, quoted under Ref. [12]), until the ratio $\varepsilon(T)/T^4$ stabilizes to a constant, as it would be the case for a gas of non interacting massless particles. In the latter case, the value of the constant is predicted to be:

$$\varepsilon = N_{eff}\frac{\pi^2}{30}T^4 \approx \frac{N_{eff}}{3}T^4$$

$$N_{eff,QGP}(n_f) \cong 8\cdot 2 + (\frac{7}{8})(4\cdot 3)n_f \ldots i.e.: \frac{N_{eff,QGP}(3)}{3} \cong 16 \qquad (5.2)$$

Lattice QCD calculations give a value around 12, about 80% of the predicted value. The deviation could be due to (expected) corrections to the relativistic perfect gas, which die only logarithmically with the increasing temperature, due to asymptotic freedom. It is unclear at the moment if the difference can be accounted by perturbative QCD calculations, or if it indicates more radical, non-perturbative departures from the perfect gas (see the Lectures by M. Gyulassy at this School[13]).

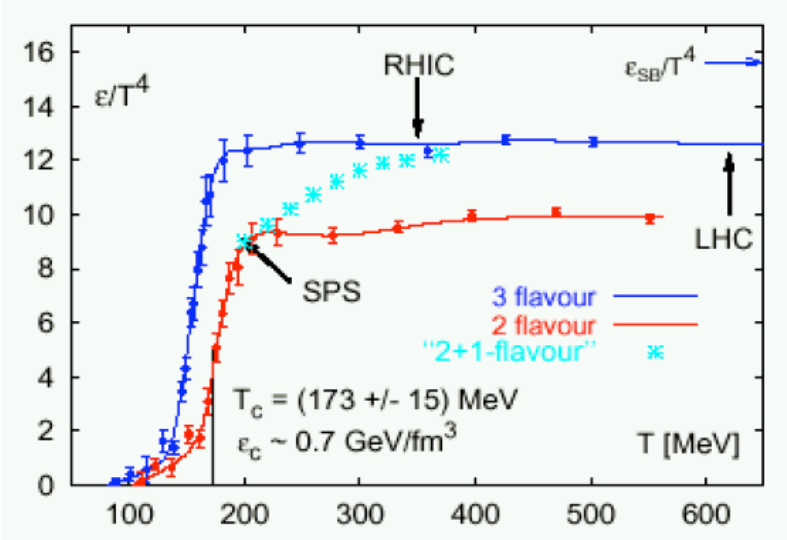

Fig. 5.4. Lattice QCD calculations of the energy density of hadronic matter vs. T (Ref. [12]).

6. Debye screening of charmonia

The spectrum of charmonium states is well reproduced by a charm-anticharm potential, which is the superposition of a Coulomb-like term (i.e. a massless gluon) and a rising, confining, term:

$$V(r) = \sigma r - \frac{\alpha_c}{r} \tag{6.1}$$

In the de-confined phase, a phenomenon analogous to Debye screening is supposed to take place, with the gluon taking a non-vanishing mass (like the photon in a Coulomb plasma). One can describe the new situation by a modified potential:

$$V(r) = \frac{\sigma}{\mu_D(T)}(1 - e^{-\mu_D(T)r}) - \frac{\alpha_c}{r} e^{-\mu_D(T)r} \tag{6.2}$$

the lattice QCD calculations described in the last Section suggest precisely this to happen. The exponential of the free-energy diverges for large r in the confined phase, corresponding to the rising term in Eq.(6.1), while it goes to a constant in the de-confined phase, corresponding to the finite range potential in (6.2).

The function $\mu_D(T)$ determines the interpolation between the two cases. μ_D vanishes below the critical temperature, and Eq. (6.2) goes back to (6.1), while it rises with T above T_c. For large enough μ_D, the screening can prevent charmonium formation. We give in the Table, see Ref. [2], the values of μ_D for which the lowest lying charmonium states become unbound and the corresponding values of the temperature, T_D.

	J/Ψ	Ψ'	χ_c(1P)
M(GeV)	3.096	3.686	3.415
r(fm)	0.89	1.5	2.0
μ_D	0.699	0.357	0.342
$T_D(n_f=3)$(MeV)	406	189	178

The J/Ψ disappears at quite higher temperatures than the critical temperature. However, a good fraction of the J/Ψ observed in absence of nuclear effects originate from the decay of higher charmonium states, about 40% from Ψ' and χ_c states which melt right above the critical temperature. Thus the estimates presented here are consistent with a sizeable reduction of J/Ψ as soon as the critical temperature is reached.

7. Summing up

The fireball produced in collisions with low energy density is essentially a pion gas thermalized at some temperature,T, below the Hagedorn temperature;

Increasing the energy density ε, by increasing the c.o.m. energy and/or centrality, several phenomena take place in succession:

- higher resonances appear in the fireball;
- due to the increasing multiplicities of higher states, it becomes more and more difficult to increase the temperature;
- we get in the Hagedorn gas limit:

$$dT/d\varepsilon \sim(\beta-\beta_c)^{3/2}$$

- hadron bags get in contact, bags fuse and quarks and gluons start being liberated.

A cartoon representing all this could be as in Fig. 7.1.

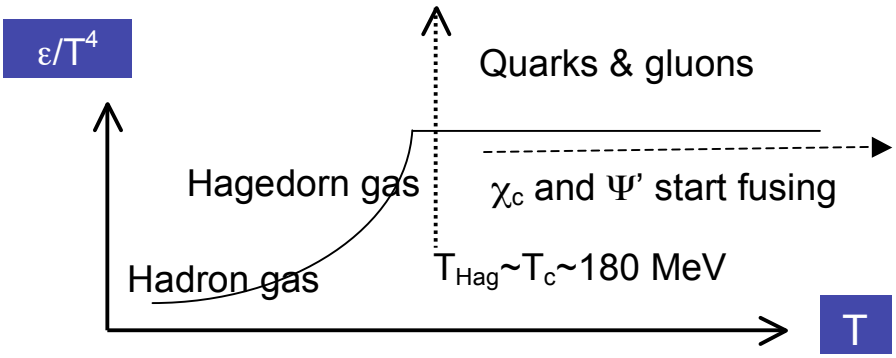

Fig. 7.1.

LECTURE 2

Summary

1. *J/Ψ dissociation cross-sections in the Constituent Quark Model*
2. *Attenuation factors*
3. *Results for the hadron and Hagedorn gases*
4. *A bold speculation*
5. *J/Ψ as a probe of QGP: some conclusions*

1. J/Ψ dissociation cross-sections in the Constituent Quark Model

I consider in this Lecture the interaction of the J/Ψ with the hadrons that can be excited from vacuum at the huge energy densities reached already at the SPS in heavy ion collisions. Each of these hadrons is able to interact with the J/Ψ, transferring its c-cbar content to open charm final states:

$$h + J/\Psi \rightarrow D_{(s)}^{(*)} + \overline{D_{(s)}^{(*)}}$$
$$(h = \pi, \eta, K, \rho, \omega, \phi)$$

Even restricting to tree-level diagrams, the interactions involve a large number of multi-meson couplings which cannot be derived from first principles, at present. Some couplings we can control from experimental data, for example the D*Dπ coupling, but for most of them we have no experimental input . One has to resort to models. Calculations available in the literature can be classified in four classes:

- perturbative QCD (pQCD) based calculations;
- quark interchange models;
- QCD sum rules calculations;
- meson exchange models.

For a nice review of these topics see Ref.[14].

The approach I shall describe is closely related to the meson exchange method. The total amplitude is written in terms of tree-diagrams involving effective trilinear and quadrilinear couplings such as:

$$g^{(3)}{}_{MD\bar{D}} = (\pi, \eta, K, \rho, ...) D\bar{D}; g^{(3)}{}_{J} = J D\bar{D};$$
$$g^{(4)}{}_{JMD\bar{D}} = J(\pi, \eta, K, \rho, ...) D\bar{D}$$

In turn, multi-meson couplings are evaluated by the so-called Constituent Quark Model, a model originally devised to compute exclusive heavy to light meson decays and tested on a quite large number of such processes[15].

The essence of the model is shown in Fig.1.1 , for the case of the $J\pi D\bar{D}$ coupling. One starts by computing the quark loop on the left-hand side, c and q being the charm and light quarks, respectively, and then equates the result with the right-hand side diagram, computed with the vector dominance ansatz:

$$j_\mu^{e.m.} = \frac{M_{J/\Psi}^2}{f_{J/\Psi}} \Psi_\mu$$

Calling $\zeta(q^2)$ the result of the Feynman diagram on the left-hand side, we derive $g_{J\pi D\bar{D}}$ from the equation:

$$\zeta(q^2) = \frac{M_{J/\Psi}^2}{f_{J/\Psi}} \frac{1}{q^2 - M_{J/\Psi}^2} g_{J\pi D\bar{D}} \qquad (1.1)$$

with both sides evaluated at $q^2=0$. I give a few details on the calculation, mainly to illustrate the parameters involved and the related uncertainties.

D meson-charm quark vertices are represented by a quark-meson coupling of the form: $\sqrt{(M_D Z_D)}\,\gamma_5$, pions appear with a pseudovector coupling, $(f_\pi)^{-1}\, k^\mu \gamma_\mu \gamma_5$, as appropriate to their nature of quasi Goldstone bosons. Quark propagators depend upon internal momenta and an additional parameter, Δ,

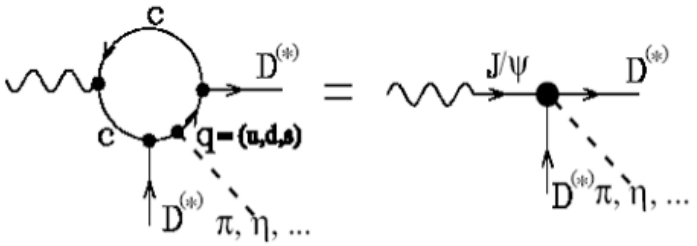

Fig. 1.1. Diagrammatic basis for the computation of $g_{J\pi DD}$.

representing the difference bewteen quark mass and the corresponding meson mass. Δ is the main free parameter of the model. It varies in the range Δ =0.3-0.5GeV for u,d quarks and 0.5, 0.6, 0.7 GeV for strange quarks[16]. The variation of results with Δ allows to estimate the theoretical error.

Integration over the internal momentum in the loop requires both an infrared and an ultraviolet cut-off. The ultraviolet cut-off , Λ, has been set to the chiral expansion scale, $\Lambda = 4\pi f_\pi$. The infrared cut-off, μ, prevents momenta to access the confinement energy region, $\mu \approx \Lambda_{QCD}$. Z_D is, essentially, the meson wave-function renormalization constant and is determined from self-energy diagrams in terms of the quark mass and the ultraviolet and infrared cutoffs[17].

The extension of pion couplings to the pseudoscalar octet is done by flavour SU(3) symmetry, ρ couplings are computed by insertion of a vector current in the quark loop and vector dominace, the extension to the other light vector mesons is done by SU(3) nonet symmetry.

In the computation of cross sections, thresholds are expressed exactly, in terms of the physical masses. Thresholds determine the energies at which the particles in the hadron gas become effective to dissociate the J/Ψ and are very relevant since they are of the same order as, sometime larger than, the thermal energies involved.

Pion cross-sections have relatively high thresholds, which disfavours them with respect to ρ s. Similarly, P-wave processes such as: π+ J/Ψ →D+ Dbar are disfavoured with respect to S-wave processes such as: π+ J/Ψ→ D* Dbar, D D*bar.

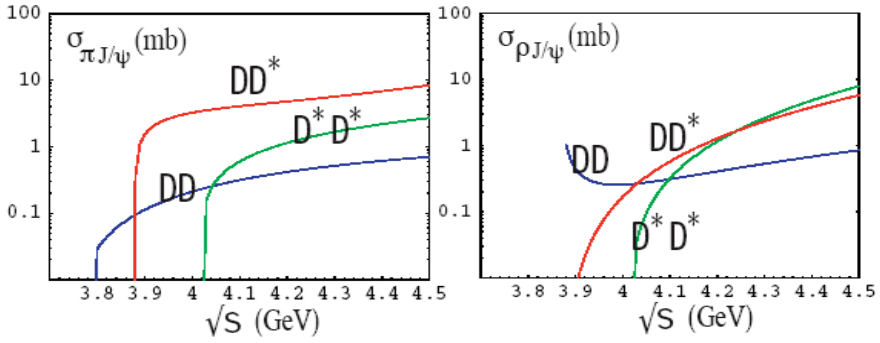

Fig. 1.2. J/Ψ dissociation cross-sections obtained in the CQM vs. c.o.m. energy

Fig. 1.2 shows the J/Ψ dissociation cross-sections obtained in the CQM as functions of c.o.m. energy[18]. Fig. 1.3 gives a compilation of the cross sections obtained with other methods, see Ref. [14].

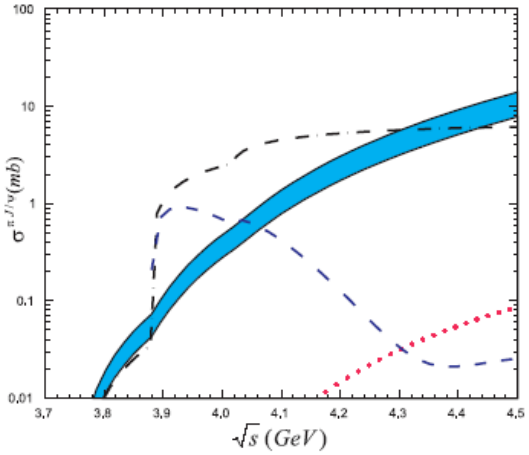

Fig. 1.3. J/Ψ dissociation cross-sections obtained with different approaches, from Ref.[14]: QCD sum rules (band), short-distance QCD (dotted line), meson-exchange models (dot-dashed lines), non-relativistic constituent quark model (dashed line).

It is reassuring to see that different approaches, all affected by their model dependencies, with the exception of the perturbative QCD calculation, give consistently non negligible dissociation cross sections:

$$\sigma_{hadr.abs.} = (1-10)\ldots mb$$

This is true, in particular for initial π's and ρ's, the most studied cases. Hadron dissociation cross sections are quite comparable to the nuclear absorption cross-section, experimentally determined[19] from p-A production of J/Ψ:

$$\sigma_{nucl.abs.} = (4.3 \pm 0.6)\ldots mb$$

In conclusion, there is a clear indication that a reliable calculation of J/ Ψ absorption needs to take into account both the effects of nuclear matter and of the hadron fireball.

2. Attenuation factors

J/Ψ produced by nucleon-nucleon collisions are detected by their decay into muon pairs. One usually gives the production rate normalized to the Drell-Yan cross section:

$$R_{J/\Psi} = \frac{\sigma(A + A \rightarrow J/\Psi + ...)}{\sigma(A + A \rightarrow \mu^+ + \mu^- + ...)}$$

Prompt muon pairs are not affected by propagation in the nuclear and hadronic medium, so that this ratio is sensitive to any mechanism which suppress the J/Ψ in the medium, that is Quark-Gluon Plasma formation as well as nuclear and hadronic absorption.

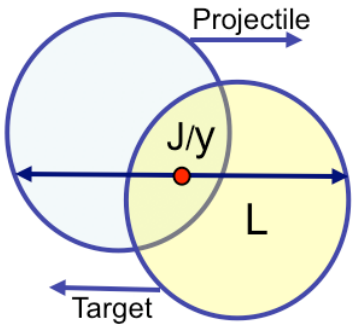

The absorption lenght in nuclear matter has been estimated by NA50 from the data on J/Ψ production in p+A collisions. The effect is parametrized by NA50 according to:

$$(R_{J/\Psi})_{nucl} = \exp(-\rho_0 \sigma_{nucl.abs.} L)$$

Fig. 2.1. The longitudinal lenght L, which regulates the nuclear J/Ψ absorption. Lorentz contraction is not reported (see text).

where:

$$\rho_0 = 0.17\, fm^{-3}$$

and L is the (average) longitudinal lenght[1] to be traversed by the J/Ψ, Fig. 2.1. Using nuclear models, NA50 gives L as function of *b*.

After traversing the nuclear matter, the J/Ψ finds itslef in the hadron fireball, which is just starting to expand. The lenght that J/ Ψ has to traverse to get out of the fireball depends, among other factors, from the direction of the J/ Ψ and the shape of the fireball. Assuming for simplicity a spherical fireball and isotropic J/Ψ, the average leght that a J/ Ψ produced anywhere inside the sphere has to traverse before escaping is:

$$l_{av.} = \frac{3}{8} l$$

where l is the transverse dimension of the fireball[2], defined in Lecture 1, see Fig. 1.1. Correspondingly, we get the attenuation factor:

---

[1] Note that the decrease of L due to the Lorentz contraction in the c.o.m. system, 1/γ, is compensated by a factor γ in the nucleon density.

[2] for a flat-disk fireball of diameter *l*, we would get a slightly different numerical factor, $l_{av.} = 4/(3\pi)l$.

$$A_{hadrons} \propto \exp[-\sum_i < \rho_i \sigma_i >_T \frac{3}{8} l]$$

where ρ_i and σ_i are densities and dissociation cross-sections of the different hadron species. The product is averaged in the thermal bath represented by the hadron gas at temperature T.

Using nuclear models, NA50 gives L as function of *b*, as shown in Fig. 2.2. Note that L flattens out around $l=2R$ (corresponding to maximum centrality, $b = 0$). If there were nuclear effects only, the ratio of J/Ψ production to Drell-Yan pairs should flatten for $l \rightarrow 2R$ (L → maximum value) while data continue to decrease at large l, as we show later. The variable *l* is better suited than L, to describe the central region and the absorption by the hadron fireball.

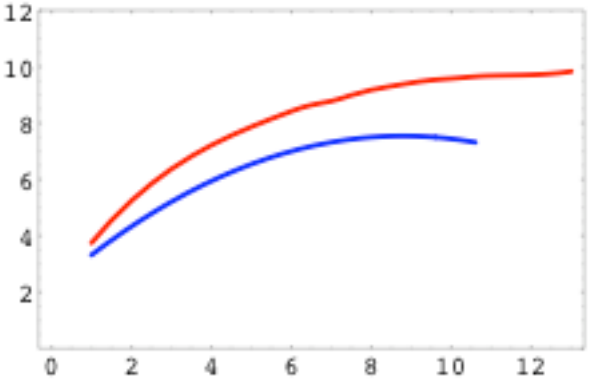

Fig. 2.2. The average longitudinal lenght L vs the centrality variable, l, for Pb (red) and for In. Note the flattening of L around the maximum value of l, correponding to central collisions.

Using further the geometrical relation: $l=2R-b$, we express L in terms of *l*, thus obtaining the total attenuation factor as function of the fireball transverse size *l*, in the form:

$$A_{Tot} = N \cdot \exp[-\rho_0 \sigma_{nucl.abs.} L(l)] \cdot \exp[-\sum_i < \rho_i \sigma_i >_T \frac{3}{8} l] \qquad (2.1)$$

The absorption lenght in the fireball is quite comparable to $\lambda_{nucl.abs.} \sim 14$ fm and the absorption increases quite strongly with temperature. We find that the contributions of vector mesons are very important, due to the low threshold of the cross-sections and to their large multiplicity. Including some other resonance like e.g. $a_1(1230)$ should not make much of a difference, since they do not present further advantages and are unfavoured by the higher mass.

3. Results for the hadron and Hagedorn gases

We fit the NA50, S-U and Pb-Pb data for $l < 5$ fm with the previous formula, including fireball absorption as function of temperature, T, as well as nuclear absorption. We find good fit for the range: 165 MeV< T<185 MeV, see Fig. 3.1.

Fig. 3.1. J/Y production normalized to Drell-Yan muon pairs vs the centrality variable *l*.NA 50 data on Pb-Pb (boxes) and S-U (stars) collisions. Superimposed the nuclear absorption curve (red) and nuclear+ fireball absorption (blue), without geometrical, centrality dependent, effects (see text).

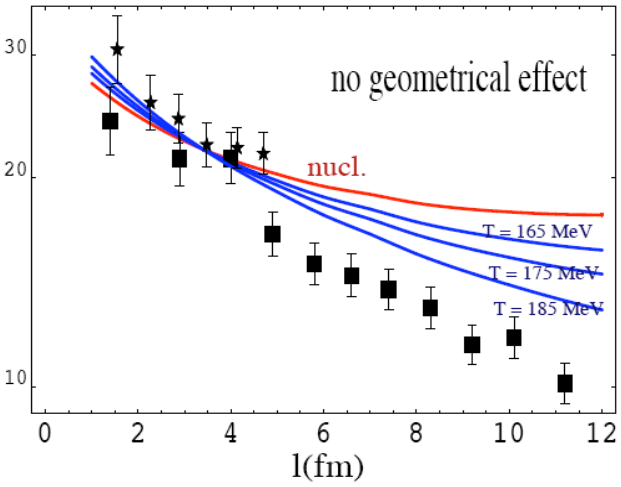

It is quite encouraging that a microscopic calculation produces a temperature which is quite consistent with everything we know about the not-so-central collisions. The fit becomes worse and worse with increasing centrality.

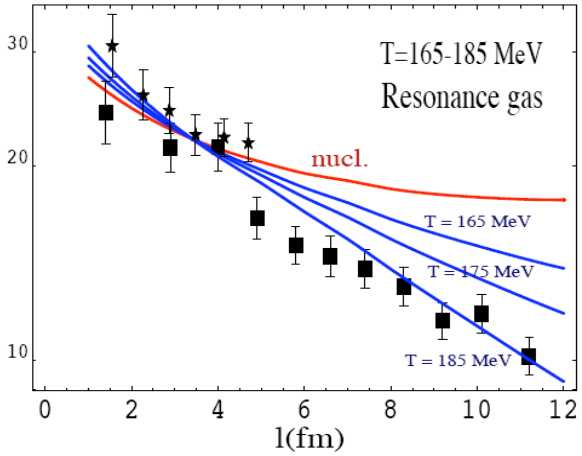

Fig. 3.2. Same as in Fig. 3. with geometrical effects taken into account.

However, we should take into account that the energy density deposited in the fireball increases with centrality. Thus we may expect that T increases with centrality and, correspondingly, the opacity becomes larger. To estimate this effect, we:

- allow an increase in energy density from l-5 fm onwards, by scaling with the factor g(*b*)=g(2*R*-*l*) introduced in Lecture 1, Sect. 1;
- use the energy density-temperature relation of the hadron gas to derive the temperature appropriate to *l* to compute the opacity.

The procedure introduces in Eq. (2.1) a further dependence from *l*, via the temperature of the thermal bath. We find curves much closer to the data, but still a marginal fit not reproducing, in particular, the discontinuity that data show around *l* =5. Even worse, the temperatures that are required at small centrality are quite large: if we start with T = 185 at *l* = 5 fm, we need to go as high as T = 205 MeV at *l* = 12 fm. It is unlikely that a hadron gas can reach these temperatures.

To analyse the situation further, we introduce the concept of a limiting temperature. Instead of using a pseudoscalar- vector Meson gas we fix the temperature for *l* < 5fm at T = 175 MeV and extrapolate to higher centrality with the above procedure applied ***to a full Hagedorn gas with T= 180 MeV***. The result is shown in Fig. 3.3. Corrections due

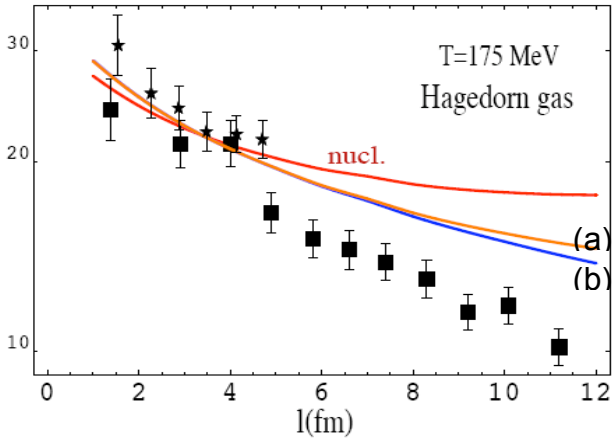

to increasing energy density with centrality are not accounted in (a) and introduced in (b).

Fig. 3.3. Same as in previous figures, assuming the fireball to be a Hagedorn gas with T_H=180 MeV. Initial temperature is fixed at T=175 MeV to fit the data for l<5fm.

The sharp rise of degrees of freedom near the Hagedorn temperature makes so that the temperature does not rise appreciably with centrality, the dissociation curve cannot become harder and the predicted absorption falls short from explaining the drop observed by NA50.

To appreciate better the significance of the effect, we plot in Fig. 3.4 the ratio Observed/Expected vs. l for the cases: (a) T(l < 5fm) =175 MeV; (b) T(l < 5fm) =185 MeV; (c) T(l < 5fm) =175 MeV, Hagedorn gas with T_H = 180 MeV.

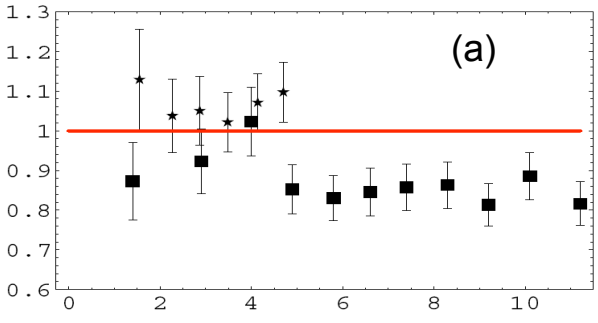

T(l<5fm) = 175 MeV
T(l=12fm)>190 MeV

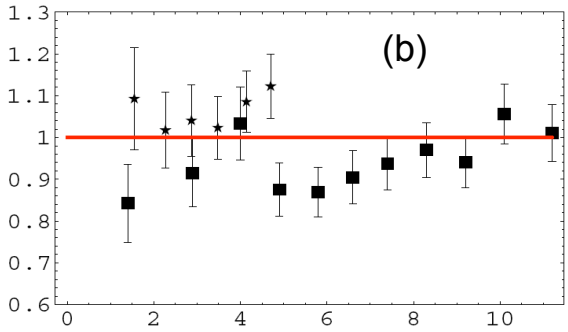

T(l<5fm) = 185 MeV
T(l=12fm)>200 MeV

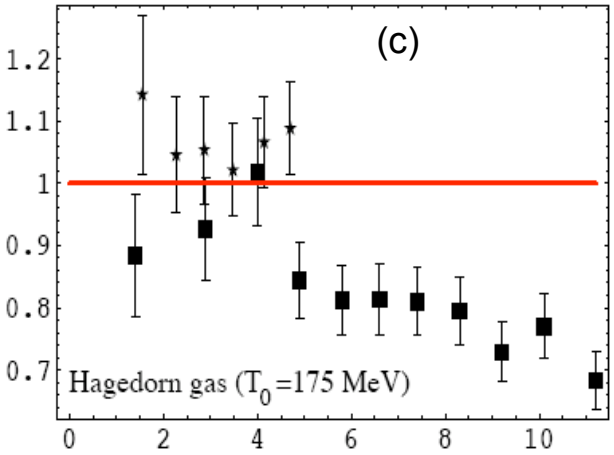

T(l<5fm) = 175 MeV
Hagedorn gas, T_H=180 MeV

Fig. 3.4. Ratio: Observed/Expected for J/Ψ production normalized to Drell-Yan muon pairs vs the centrality variable l. NA 50 data on Pb-Pb (boxes) and S-U (stars) collisions. Figs. (a) and (b): fireball is a pseudoscalar + vector meson gas, with initial temperatures (for l<5fm) as indicated; also indicated the temperatures reached at l=12fm; (c) Hagedorn gas with T_H=180 MeV, initial temperature T=175 MeV.

Some comments. The curve shown in Fig. 3.4 (c) embodies the limiting absorption from a hadron gas, anything harder could be due to the dissociation of the J/Ψ in the quark-gluon plasma phase. We must stress, however, that J/Ψ dissociation due to higher resonances than vector mesons has been neglected. The decreasing couplings of the higher resonances could eventually resum up to a significant effect, which would change the picture. Something similar happens e.g. in deep inelastic scattering, where the cross section due to any individual resonance falls down because of its form factor, but the total cross section is mantained by the new resonances appearing at larger values of the energy. However, the underlying reason for this is that we are entering a regime in which the phenomenon is described by a new picture, namely the scattering off elementary partons. In our case, this would mean going over to a description where charmonium dissociation is due to the interaction with quarks and gluons, which is precisely the signal of the deconfined plasma, above the Hagedorn temperature.

4. A bold speculation

Going back to Fig. 5.4 in Lecture 1, it is tempting to interpret the rise of ε/T^4 as due to the excitation of more and more hadron resonances, as it happens in the Hagedorn gas. The transition starts when the number of effective degrees of freedom in the hadron gas equals approximately the degrees of freedom of a gas of quarks and gluons. For a Hagedorn gas with T_H=180 MeV, the transition temperature and energy density are numerically found to be:

$$\varepsilon(T)/T^4 \approx 12 \Leftrightarrow T = T_{trans} = 168\,MeV;\ldots\varepsilon(T_{trans}) = 2GeV/fm^3 \qquad (4.1)$$

The value of the energy density agrees with what can be estimated from the Bjorken formula, Lecture 1. Encouraged by this, we may assume, as a bold hypothesis, that Pb-Pb collisions at l = 5 fm produce a fireball with exactly ε = 2 GeV/fm^3. For l > 5fm we may trasform the lenght scale in Fig. 3.4 (c) into an energy density scale, by scalig the energy density with the geometrical factor g(b).

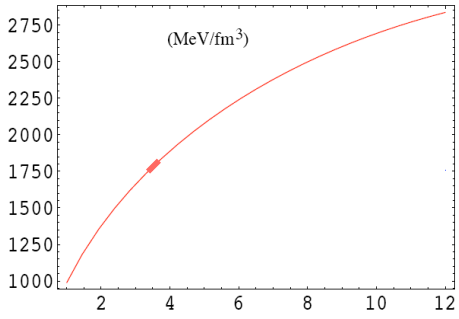

Fig. 4.1. Energy density, according to the Bjorken formula, vs. the centrality variable l, as obtained from the geometrical function g(b). Normalization is given by the assumption that ε=2 GeV/fm^3 for l = 5 fm.

Recall that g(b) embodies the increase of the nucleon surface density with increasing centrality. Fig. 4.1 gives the l-ε relation implied by g(b) and Fig. 4.2 gives the result of the recalibration: the ratio Observed/Expected for J/Ψ given as a function of the energy density. For l>5 fm we may also transform

energy densities into temperatures, using the relation: $T \approx (\varepsilon/12)^{1/4}$, approximately valid above the transition point. We have indicated in Fig. 4.2 the temperatures at which Ψ' and χ states melt, according to the results presented in Sect. 6 of Lecture 1. The reduction of 20-30% in the expected J/Ψ yield is quite compatible with the disappearence of these states.

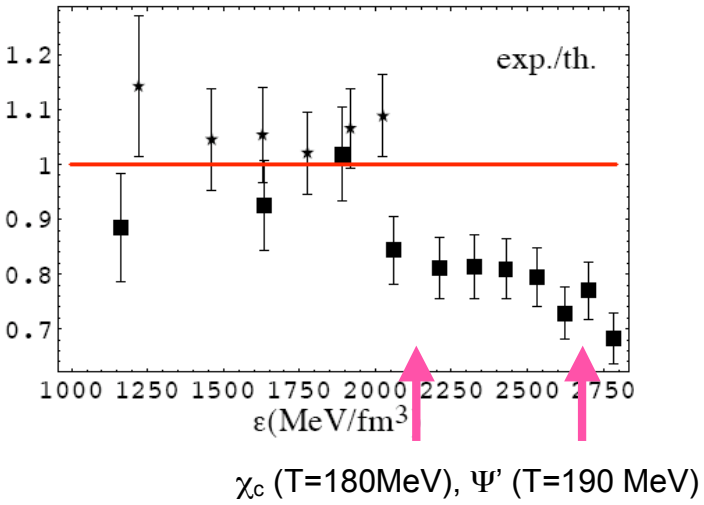

Fig. 4.2. The ratio: Observed/Expected for J/Ψ production normalized to Drell-Yan muon pairs vs the energy density ε. NA 50 data on Pb-Pb (boxes) and S-U (stars) collisions.
The fireball is assumed to be a Hagedorn gas with initial temperature T=175MeV and T_H=180 MeV. Arrows indicate the temperatures where χ_c and Ψ' melt, according to the Table in Lecture 1, sect. 6.

5. J/Ψ as a probe of QGP: some conclusions

When the idea was proposed, it was believed that J/Ψ would suffer little absorption from nuclear matter and from the "comoving particles" (σ<1 mb), hence that there would be very little background to the QGP signal;

Nuclear absorption measured from p-A cross sections (but uncertainties still remain!) is instead ~ 4-5 mb, with a corresponding attenuation lenght ~ 14 fm and therefore a signal-to-noise ratio ~ 1. Absorption cross sections by comoving particles point also to the few mb range, as has been estimated with several methods involving rather different approximations.

In the work I have described in these Lectures, we have made a new calculation of the J/Ψ dissociation cross-sections by pseudoscalar and vector mesons in a reliable model tested in other processes (the Quark Constituent Model) and we have applied the results to a hadron gas made of these particles.

The effects of comovers are (i) non negligible and (ii) strongly temperature dependent.

If we allow temperatures in excess of 200 MeV in this hadron gas, we can fit the NA50 results, albeit marginally.

On the other hand, if we accept that there is a limiting temperature to the hadronic phase, estimated to be 170-180 MeV from independent sources (hadron spectrum, lattice QCD calculations) comovers ***cannot explain*** the drop in J/Ψ production seen at large centralities by NA50.

The picture that QGP sets in at centrality $l \sim 5$ fm is consistent with known temperature and energy density ranges. The observed drop in J/Ψ would be due first to χ_c and, later, to Ψ' melting.

The limiting temperature being a quite reasonable assumption, we conclude that the SPS has most likely seen the QGP. It would be interesting to correlate the J/Ψ signal to the other hint of new phase seen at the SPS, namely the increase in strangeness production. This has not been done, thus far, but work is in progress.

RHIC data on J/Ψ would be extremely valuable, to check the signal against other signatures and so would the beauty signal. LHC data are eagerly wanted !

The study of charmonia in QGP is not concluded with the demonstration that QGP exists. The level spectrum vs. T could give interesting information on the dynamics of quark and gluons, on the non-perturbative corrections to the picture of a free quark gluon gas and it would probe deeply the new phase of matter.

REFERENCES

[1] T. Matsui and H. Satz, Phys. Lett. **B178**, 416 (1986).

[2] For a review see e.g. R. Vogt, Phys. Rep. **C 310** (1999) 197.

[3] L. Maiani, F. Piccinini, A.D. Polosa, V. Riquer, Nucl. Phys. **A 741** (2004) 273; **A 748** (2005) 209.

[4] For a recent and extended review see: U. Heinz, Concepts of Heavy-Ion Physics, lecture Notes, hep-ph/0407360.

[5] M.C. Abreu et al., Phys. Lett. **B450**, 456 (1999); M.C. Abreu et al., Phys. Lett. **B477**, 28 (2000). Latest analysis: http://na50.web.cern.ch/NA50.

[6] J. D. Bjorken, Phys. Rev. **D27** (1983) 140.

[7] See e.g. J. L. Goity and H. Leutwyler, Phys.Lett.B228 (1989) 517.

[8] E791 Collaboration (E.M. Aitala et al.) Phys. Rev. Lett. **89** (2002)121801.

[9] SPS data have been analysed recently in F. Becattini, A. Keranen, L. Ferroni, T. Gabbriellini, nucl-th/0507039; for RHIC data see P. Braun-Munzinger, D. Magestro, K. Redlich , J. Stachel Phys. Lett. **B518** (2001) 41.

[10] J. Letessier, J. Rafelski, Hadrons and Quark–Gluon Plasma, Cambridge Monogr. Part. Phys. Nucl. Phys. Cosmol.,vol.18, 2002.

[11] N. Cabibbo, G. Parisi, Phys. Lett. **B59** (1975) 67.

[12] F. Karsch, Lattice QCD at High Temperature and Density, hep-lat/0106019.

[13] M. Gyulassy, in these Proceedings.

[14] T.Barnes, Charmonium Cross Sections and the QGP, nucl-th/0306031.

[15] A. Deandrea, N. Di Bartolomeo, R. Gatto, G. Nardulli
and A.D. Polosa, Phys. Rev**. D58** (1998) 034004 (1998); See also A.D. Polosa,``The CQM Model'', Riv. Nuovo Cim. Vol. 23, N. 11 (2000).

[16] A. Deandrea, R. Gatto, G. Nardulli, N.A. Tornqvist, Phys. Lett. **B502** (2001) 79.

[17] D. Ebert, T. Feldmann, R. Fredrich, H. Reinhardt, Nucl. Phys B434 (1995) 619

[18] see the second paper quoted in [3].

[19] B. Alessandro et al., NA50 Collaboration, Nucl. Phys. **A715** (2003) 679c.